

# SuperKEKB IR UPGRADE IDEA WITH $\text{Nb}_3\text{Sn}$ QUADRUPOLE MAGNETS

M. Masuzawa<sup>†</sup>, K. Aoki, Y. Arimoto, H. Koiso, A. Morita, N. Ohuchi, M. Tobiya, KEK, Tsukuba, Japan

## Abstract

SuperKEKB is an energy-asymmetric double-ring collider with an electron beam energy of 7 GeV and a positron beam energy of 4 GeV [1]. An extremely small beta function at the interaction point (IP) and low emittance are necessary to achieve a peak luminosity that is an order of magnitude higher than that achieved by the KEKB. Superconducting magnets provide the focusing magnetic field required to squeeze down the beta functions at the IP. The Belle II detector solenoid field is fully compensated for by the superconducting solenoids and the compensation solenoids on each side of the IP.

Modification of the superconducting magnet system and interaction region (IR) is a potential upgrade item needed to further improve the SuperKEKB performance. The new IR design concept and technical challenges of superconducting magnets with  $\text{Nb}_3\text{Sn}$  cables are described in this paper.

## INTRODUCTION

The SuperKEKB IR is designed to achieve extremely small beta functions at the IP,  $\beta_x^*$  and  $\beta_y^*$  in the horizontal and vertical directions, respectively. Figure 1 shows the conceptual layout of the QCS magnets, the final focusing superconducting magnets [2]. QC1s and QC2s provide the vertical and horizontal focusing fields, respectively. The QCS magnets consist of eight quadrupole magnets, 35 corrector magnets for beam tuning, eight magnets for leak field cancellation, and four solenoids: ESL, ESR1, ESR2, and ESR3.

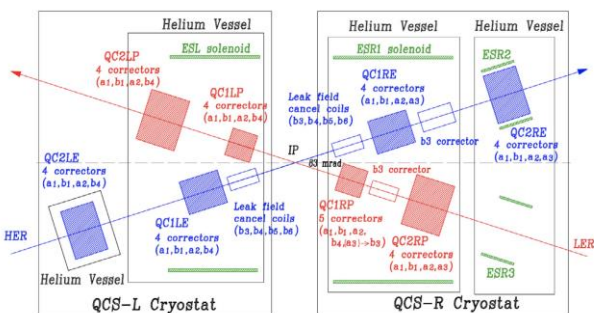


Figure 1: Layout of the QCS magnets.

The solenoid field of Belle II is fully compensated for by ESL, ESR1, ESR2, and ESR3.

$$\int_{IP} B_z(s)ds = 0, \quad (1)$$

<sup>†</sup>mika.masuzawa@kek.jp

where  $B_z$  is the magnetic field along the virtual beam axis through the IP and  $s$  is the distance from the IP. The X-Y coupling and the horizontal and vertical dispersions are corrected to be zero at the IP using skew quadrupole magnets and horizontal and vertical dipole magnets on each side of the IP. In the LER, the chromatic X-Y coupling arising from the solenoid field overlapping QC1s is corrected using rotatable sextupole magnets. The finite crossing angle between the beam orbits and solenoid axis causes vertical dispersion. This results in a vertical emittance that is strongly dependent on the transverse component of the magnetic field along the orbit, as represented by  $B_x(s)$ ,

$$B_x(s) \cong -\frac{x}{2}B'_Z(s) = -\frac{s\phi}{2}B'_Z(s). \quad (2)$$

A half crossing angle  $\phi$  or/and  $B'_Z(s)$  should be decreased to reduce the vertical emittance. Because decreasing half crossing angle  $\phi$  requires a complete change of the IR, we focused on modifying  $B_z(s)$  such that its differential along the beam trajectory  $B'_Z(s)$  became smaller than that in the present system.

## NEW IR

The new design concept of the IR upgrade involves making the beam trajectory as parallel to the QC1 magnet axis as possible, cancelling the X-Y coupling and its chromaticity between the IP and QC1 as close to zero as possible and minimizing  $\varepsilon_y$ , by redesigning the  $B_z(s)$  profile. The vertical offsets and rotations of QC1P and QC2P and the horizontal offsets of QC1E and QC2E are expected to be considerably smaller than the present values with the new compensation solenoid field design and the incorporation of magnetic yokes on QC1P.

## Magnetic Field Profile

The design concepts of the new IR are listed as follows:

- Separating QC1P from the solenoid compensation system by adding a new compensation solenoid between the IP and QC1, as shown in Fig. 2.
- QC1P relocation, closer to the IP by 100 mm (the distance between the IP and the magnet center "L\*" being present 935 mm to 835 mm), as is indicated in Fig. 3.

The magnetic field profile was calculated using Opera3D, where the magnetic field generated by the Belle II solenoid coil is included. As shown in Fig. 4, the peak field is lower with the new IR than with the present IR, which allows for the use of thinner coils. With the new compensation solenoid coil, the Belle II detector solenoid field is compensated between IP and QC1P. Some parts of the cryostat and Belle II detector interfere on the forward side. The boundary of the detector must be determined to proceed with the discussion of the IR installation method.

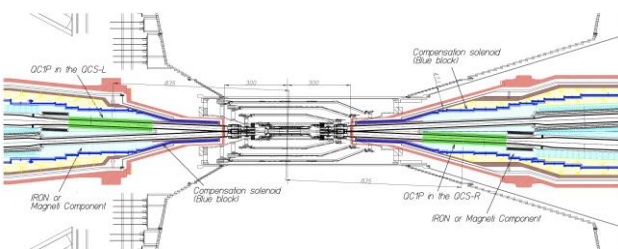


Figure 2: New QCS is shown. The compensation solenoid coils and QC1P magnets are indicated in blue and green, respectively.

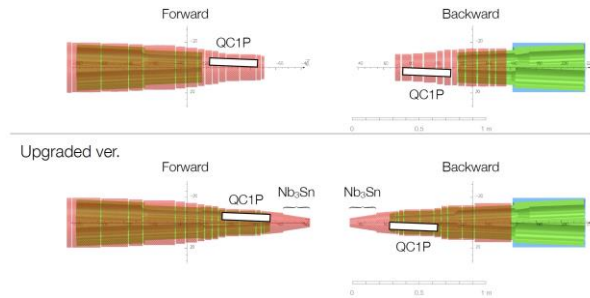


Figure 3: The QC1P position comparison. The top figure shows the present, and the bottom figure shows the new IR, respectively.

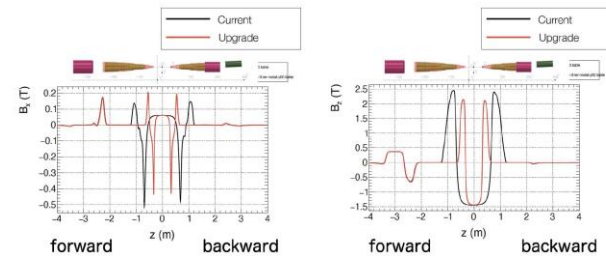


Figure 4: Comparison between the present (black) and the new (red) compensation solenoid field profile of  $B_x$  and  $B_z$ . The “forward” and “backward” in the plots correspond to the QCS-R and QCS-L in Fig. 1, respectively.

### Optics Evaluation

A preliminary optics evaluation was conducted, focusing on the effects on the dynamic aperture and Touschek lifetime, chromatic coupling, and vertical emittance. Neither beam-beam effects nor octupole corrections were included in this evaluation, nor did it include the effects of ESR3 and the magnetic shield gap. Figure 5 compares the dynamic aperture and Touschek lifetime for LER when  $\beta_y^*$  is 0.27 mm. By relocating the QC1P 100 mm closer to the IP, the Touschek lifetime increased from 261 s to 424 s. Chromatic X-Y coupling parameters,  $\partial R_1/\partial\delta$ ,  $\partial R_2/\partial\delta$ ,  $\partial R_3/\partial\delta$  and  $\partial R_4/\partial\delta$  are obtained with the new IR and it was found that they become a few orders of magnitude smaller with the new IR.

The present and new IR orbits and beta functions are shown in Fig. 6. The orbit displacement with new IR lattice is  $\sim 10 \mu\text{m}$  at QC1, while it is about 1 mm with the present lattice. The vertical emittance from the new IR was calculated to be 14 fm, which is negligible.

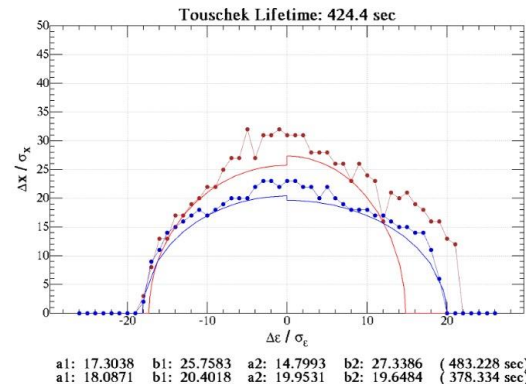
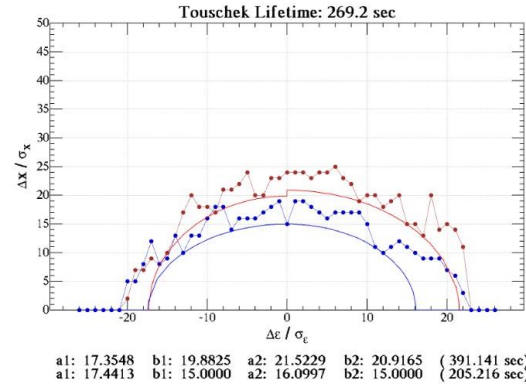


Figure 5: Comparison between the present (top) and the new (bottom) IR lattice when  $\beta_y^* = 0.27$  mm.

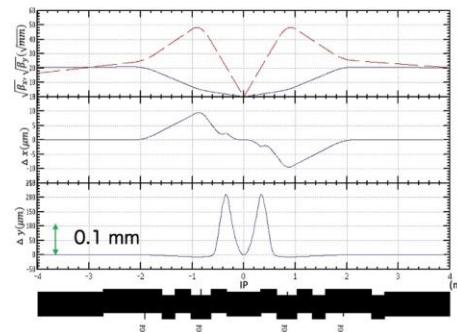
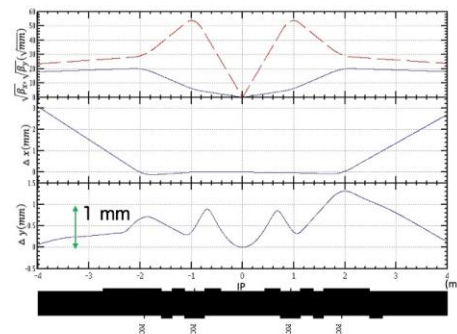


Figure 6: The beta functions and the orbit: present (top) and new (bottom) IR lattice when  $\beta_y^* = 0.27$  mm.

## New QC1 with $Nb_3Sn$ Cable

QC1P relocation requires a 12% increase in the field strength if the magnetic length is maintained. This corresponded to an increase in the field gradient from 68 T/m to 76 T/m. The current density of the new QC1P superconducting cable must be increased to higher than  $3000\text{A/mm}^2$ , which is twice that of the current QC1P. The field distribution in the QC1P coil was evaluated at the center along the beam direction, as shown in Fig. 7. The maximum field experienced by the coil was approximately 2.5 T and the current density in the coil was  $3112\text{A/mm}^2$ , which was difficult to achieve using an NbTi coil. Therefore, a superconducting wire that can withstand a higher current density than that of NbTi is required.  $Nb_3Sn$  is known to have a higher critical current density and temperature than NbTi [3]. Current sharing temperature is compared in Fig. 8 for NbTi and  $Nb_3Sn$ .  $Nb_3Sn$  exhibited a larger temperature margin than NbTi for maintaining the superconducting condition at a current density of  $3000\text{A/mm}^2$ . A new QC1P using a  $Nb_3Sn$  wire is now being studied, and intensive R&D work is being conducted to check whether  $Nb_3Sn$  can be used for QC1 magnets. Many studies have been conducted on accelerator magnets based on  $Nb_3Sn$  technologies, and actual magnets have been manufactured [4], although they are much larger magnets and operate at a higher magnetic hygiene, such as  $\sim 11\text{T}$ .

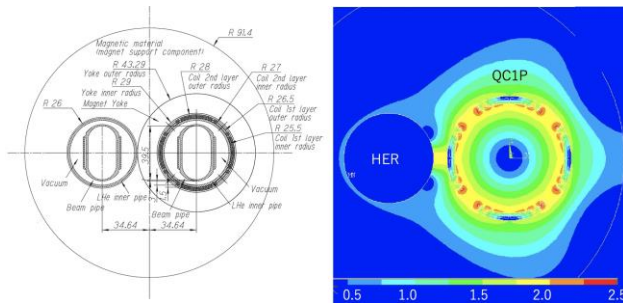


Figure 7: 2D Field evaluation for QC1P.

Research has been conducted on wires to determine the most appropriate wire and filament size, establish heat treatment procedures, measure critical currents and critical temperatures, develop quench protection systems, etc.  $Nb_3Sn$  wires are brittle and sensitive to strain, and their superconducting properties may change significantly with strain and heat treatment processes. We plan to design and fabricate coil-winding jigs by performing the first coil winding, impregnation, and heat treatment. The superconducting, mechanical, and magnetic properties will be evaluated. Data on the coil and magnet production errors must also be obtained. We focus on feasibility testing to determine whether QC1 can be fabricated using  $Nb_3Sn$ , which is essential for new IR magnet system design.

## SUMMARY

A new IR optics idea was evaluated using a 3D magnetic field profile. To summarize, 1) the dynamic aperture and Touschek lifetime are improved, 2) the chromatic X-Y coupling improves significantly, and 3) the contribution to

the vertical emittance from the IR is in the order of several tens of femtometers. Therefore, machine tuning is expected to become easier with new IR. QC1 and the new compensation solenoid coil must be designed in a more compact manner, which requires the use of  $Nb_3Sn$  wire. Research and development on  $Nb_3Sn$  magnets is essential for realizing the IR upgrade idea.

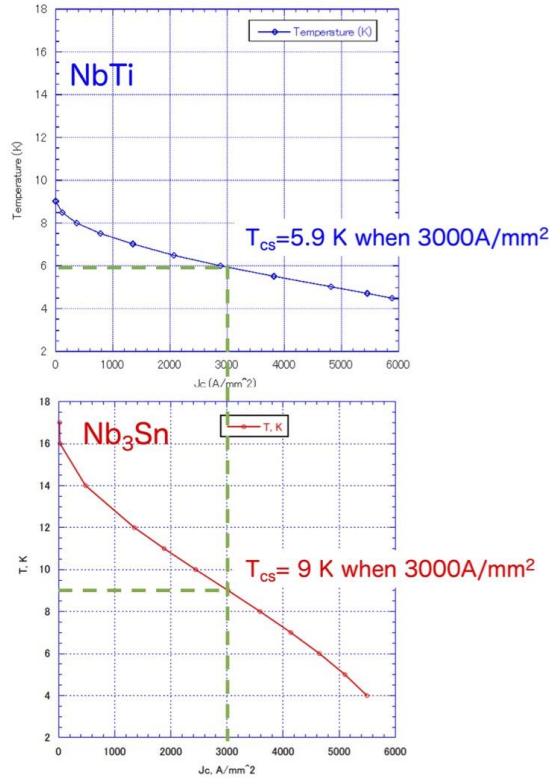


Figure 8: Current sharing temperature as a function of current density for NbTi (top) and  $Nb_3Sn$  (bottom).

## REFERENCES

- [1] K. Akai, K. Furukawa, and H. Koiso, "SuperKEKB collider," Nucl. Instrum. Methods Phys. Res., Sect. A, vol. 907, pp. 188–199, Nov. 2018. doi:10.1016/j.nima.2018.08.017
- [2] N. Ohuchi et al., "SuperKEKB beam final focus superconducting magnet system," Nucl. Instrum. Methods Phys. Res., Sect. A, vol. 1021, p. 165930, Jan. 2022. doi:10.1016/j.nima.2021.165930
- [3] E. Barzi and A. V. Zlobin, " $Nb_3Sn$  Wires and Cables for High-Field Accelerator Magnets," in Particle Acceleration and Detection, 2019, pp. 23–51. doi:10.1007/978-3-030-16118-7\_2
- [4] D. Schoerling and A. V. Zlobin, Eds.,  $Nb_3Sn$  Accelerator Magnets: Designs, Technologies and Performance. Springer International Publishing, 2019. doi:10.1007/978-3-030-16118-7.